



Tubular ceramic-supported sol-gel silica-based membranes for flue gas carbon dioxide capture and sequestration

G. Xomeritakis^{a,*}, C.Y. Tsai^b, Y.B. Jiang^c, C.J. Brinker^{a,c,**}

^a Center for Microengineered Materials and Department of Chemical and Nuclear Engineering, The University of New Mexico, Albuquerque, NM 87131, USA

^b T3 Scientific LLC, 91st Avenue NE, Suite 101, Blaine, MN 55449, USA

^c Sandia National Laboratories, Advanced Materials Laboratory, 1001 University Blvd. SE, Suite 100, Albuquerque, NM 87106, USA

ARTICLE INFO

Article history:

Received 18 March 2009

Received in revised form 14 May 2009

Accepted 17 May 2009

Available online 23 May 2009

Keywords:

Sol-gel

Silica membrane

Carbon dioxide separation

Flue gas

Amine functionalization

Nickel doping

ABSTRACT

Pure, amine-derivatized and nickel-doped sol-gel silica membranes have been developed on tubular Membralox-type commercial ceramic supports for the purpose of carbon dioxide separation from nitrogen under coal-fired power plant flue gas conditions. An extensive synthetic and permeation test study was carried out in order to optimize membrane CO₂ permeance, CO₂:N₂ separation factor and resistance against densification. Pure silica membranes prepared under optimized conditions exhibited an attractive combination of CO₂ permeance of 2.0 MPU (1 MPU = 1 cm³(STP) cm⁻² min⁻¹ atm⁻¹) and CO₂:N₂ separation factor of 80 with a dry 10:90 (v/v) CO₂:N₂ feed at 25 °C. However, these membranes exhibited flux decline phenomena under prolonged exposure to humidified feeds, especially in the presence of trace SO₂ gas in the feed. Doping the membranes with nickel (II) nitrate salt was effective in retarding densification, as manifested by combined higher permeance and higher separation factor of the doped membrane compared to the pure (undoped) silica membrane after 168 h exposure to simulated flue gas conditions.

© 2009 Elsevier B.V. All rights reserved.

1. Introduction

Membrane-based gas separations gain considerable growth due to the benefits of low capital costs, low energy requirements and ease in operation. Present industrial-scale applications of gas separation membranes include carbon dioxide removal from natural gas and hydrogen purification in refinery operations [1]. Most commercial-scale membranes are polymer-based spiral-wound or hollow-fiber type devices, while ceramic or metallic membranes find applications in smaller duty separations. Polymeric membranes separate gases based on the solution-diffusion mechanism and are typically limited by the well-known tradeoff between permeability and selectivity [2]. Current development efforts in the area focus on new high-performance polymers or the design of mixed-matrix systems comprising of a molecular sieve guest phase dispersed in a continuous polymer host matrix [3].

An emerging opportunity for large-scale membrane gas separations is the capture of greenhouse gases such as carbon dioxide from the emissions of coal-fired power plants [4]. Current commercial

process employed in this area is amine absorption which is energy and capital-intensive and environmentally hazardous because of the corrosive nature of the solvents involved in the process [5]. A membrane-based carbon dioxide capture process would mitigate these issues provided that suitable membrane materials are available that can meet the requirements of treating large volumes of gas under low driving force and producing high purity carbon dioxide to inject underground [6,7].

Currently available commercial polymer membranes such as cellulose acetate do not meet the performance requirements for economical capture of CO₂ from flue gas (e.g. CO₂ permeance >2 MPU and CO₂:N₂ selectivity >80) [8]. An alternative class of membrane materials that could be used in CO₂:N₂ separation is inorganic microporous molecular sieves such as zeolites, carbons and sol-gel silicas [9]. Certain large-pore zeolites such as FAU have been reported to exhibit sufficient CO₂:N₂ selectivity [10] while molecular sieve carbons are also good candidates for this application [11]. The main challenge however is to fabricate these materials as thin membranes on large-area modules at reasonable cost, while avoiding formation of cracks that would compromise separation efficiency [12].

Chemical vapor deposition (CVD) or sol-gel derived microporous silicas are also good candidates for application in flue gas CO₂ capture, provided their amorphous structure is engineered to optimize CO₂ permeance and CO₂:N₂ selectivity [4]. So far these membranes are known to efficiently separate H₂ from larger gas

* Corresponding author. Present address: UOP LLC, 25 E. Algonquin Rd., Des Plaines, IL 60017, USA. Tel.: +1 847 391 2391; fax: +1 847 391 3736.

** Corresponding author. Tel.: +1 505 272 7627; fax: +1 505 272 7336.

E-mail addresses: george.xomeritakis@uop.com (G. Xomeritakis), cjbrink@sandia.gov (C.J. Brinker).

molecules at elevated temperatures [13,14] or CO₂ from CH₄ at ambient temperature (*T*) [15], relevant to purification of natural gas from corrosive acid gas contaminants. Current efforts in the field of sol–gel silica membranes include pore size engineering by molecular templating [16–19] and introduction of chemical functionality to improve CO₂ affinity of the membrane [20,21].

The objective of this study is to explore the separation performance and stability of sol–gel silica-based membranes for CO₂ removal under flue gas conditions. An extensive synthesis of both pure and amine-derivatized silica membranes was carried out, aiming to achieve combined high CO₂ permeance and high CO₂:N₂ selectivity, necessary for economical membrane-based flue gas CO₂ capture. The effects of operating temperature, feed humidity content and presence of flue gas contaminants such as SO₂ on membrane performance were investigated. The possibility of retarding densification phenomena by metal oxide doping was also studied. This study was motivated by the combination of several attractive features such as good processibility, pore size control and low cost of precursor materials [22], which make silica membranes a good candidate for future applications in carbon dioxide capture in power generation.

2. Experimental

2.1. Membrane support

Two types of commercial porous alumina-based supports were employed in this study. The most commonly employed support was a commercial Membralox tube of 10 mm OD, 7 mm ID and asymmetric pore structure with a final 50-Å pore γ-Al₂O₃ top layer (Pall Corp., part no. S700-00117). The 250-mm long support was cut in 5-cm long segments with a diamond wafering blade (Buehler) before membrane deposition. Occasionally, we also performed membrane deposition on a 20-nm Anodisk support (Whatman, UK) as described in detail in a previous article [23].

2.2. Mesoporous silica sublayer

A 25-Å pore surfactant-templated silica sublayer was deposited on the surface of both the Membralox and the Anodisk supports in order to provide a smooth pore size transition between the support and the final microporous silica gas separation membrane. The details of the 2-step surfactant-silica sol preparation can be found in previous publications [15]. The final molar composition of the sol was: 1 Si–22 EtOH–5 H₂O–0.004 HCl–0.08 Brij56. In the case of the Anodisk support, the sol was further diluted with equal volume of ethanol prior to casting.

2.3. Aminosilica sol preparation

For preparation of amine-derivatized silica membranes, three main sol recipes were employed, designated as aSi-*n* in the order of decreasing H⁺:–NH₂ molar ratio in Table 1. In all three recipes, the alkoxy silane precursors (TEOS = tetraethylorthosilicate, APTES = 3-aminopropyltriethoxysilane, Aldrich) were first added to ethanol and then stirred until homogeneous. Subsequently H₂O and HCl

were added and the sol was shaken for 15 min and then aged for 24 h at 25–50 °C without agitation. A high H⁺:Si molar ratio was necessary to prevent premature gelation of the sols due to the high reactivity of APTES with H₂O [20]. For recipe aSi-3 with the lowest H⁺:–NH₂ molar ratio, the initial EtOH–TEOS–APTES mixture was chilled to –20 °C before H₂O and acid were added in order to retard premature gelation reactions. No aging step was used in this case since the sol would turn turbid due to particulate silica precipitation after about 30 min at room temperature.

2.4. Pure silica sol preparation

For preparation of pure silica membranes we adopted a modified version of the recipe reported by Verweij and coworkers: 1 Si:3.8 EtOH:6.4 H₂O:8.5 × 10^{–2} HNO₃ [24]. However in our study we found that optimal membrane performance was achieved by 10-fold decrease of the amount of acid. As seen in Table 1, for recipe Si-1 the reactants were stirred for 3 h at 60 °C and then 1 volume of sol was diluted with 2 volumes of ethanol prior to membrane casting. For recipe Si-2 the reactants were shaken for 15 min and then aged for 24 h at 25–50 °C without agitation.

2.5. Nickel doping

Doping of nickel ions in the silica membrane was achieved by adding nickel (II) nitrate hexahydrate salt (Ni(NO₃)₂·6H₂O, Aldrich) to a mixture of H₂O and HNO₃. This mixture was then added to the EtOH:TEOS mixture prior to skaking and aging. The typically employed Ni:Si molar ratio was 0.1 although we attempted a few preparations with twice the Ni loading in the doped sol.

2.6. Membrane deposition

Deposition of sublayer and membrane on the tubular Membralox or Anodisk supports was carried out by dip- or spin-coating, as described in details elsewhere [20,23]. All sols were purified with 0.2 μm syringe filters prior to casting. The xerogel membrane films were calcined for 3 h at 500 °C in air (for the mesoporous sublayer) or at 300–500 °C in vacuum (for the microporous membranes). All heating and cooling steps were controlled at 1 °C min^{–1}.

2.7. Membrane permeation

Pure and mixed gas permeation studies of the Anodisk and Membralox supported membranes were carried out in our in-house permeation system as described elsewhere [20,23]. For permeation at elevated *T* (up to 100 °C), the tubular permeation cell was wrapped with heating tape and heated with a Variac transformer. A type K thermocouple (Omega) inserted in the annulus of the tubular membrane was used for temperature readout. The % humidity level in the feed was controlled by passing a certain flow rate of N₂ through a water saturator maintained at ambient *T*. The total feed (CO₂:N₂) and sweep gas (He) flow rates were 100 cm³(STP) min^{–1}. All mixed gas permeation tests were carried out at ambient feed and sweep gas pressure.

Table 1

Typical amine-silica and pure silica sol recipes used for membrane deposition in this study.

Recipe	Molar composition	Reaction condition
aSi-1	0.2 NH ₂ :1 Si:22 EtOH:5 H ₂ O:0.4 HCl	15 min agitation at 25 °C, then 24 h aging at 25–50 °C
aSi-2	0.2 NH ₂ :1 Si:22 EtOH:3.3 H ₂ O:0.2 HCl	15 min agitation at 25 °C, then 24 h aging at 25–50 °C
aSi-3	0.2 NH ₂ :1 Si:44 EtOH:3.3 H ₂ O:0.067 HCl	20 min agitation while warming from –20 to 25 °C
Si-1	1 Si:3.8 EtOH:6.4 H ₂ O:8.5 × 10 ^{–3} HNO ₃	180 min stirring at 60 °C under reflux
Si-2	1 Si:22 EtOH:6.4 H ₂ O:8.5 × 10 ^{–3} HNO ₃	15 min agitation at 25 °C, then 24 h aging at 25–50 °C

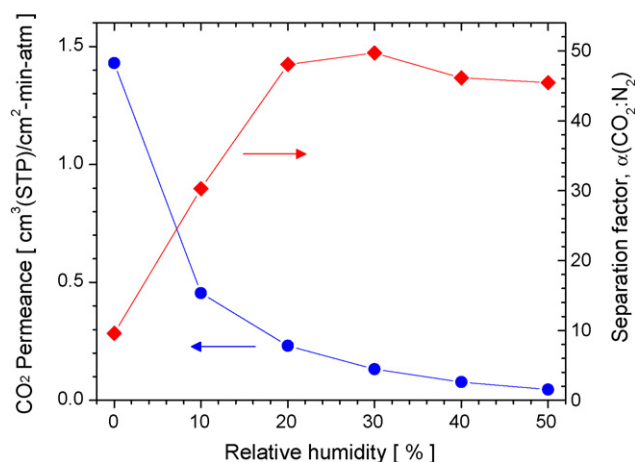


Fig. 1. Mixed gas separation performance at 22 °C of a tubular aminosilica membrane prepared with recipe aSi-1. The feed was a 10:90 (v/v) $\text{CO}_2:\text{N}_2$ mixture.

2.8. Simulated flue gas (SFG) treatment

Prolonged exposure of the membrane to SFG conditions was carried out either inside the stainless steel permeation cell or in a separable pyrex holder heated at 60–80 °C by an external heating tape. The humidified feed (50% R.H.) of 10% CO_2 in N_2 was introduced at a rate of $100 \text{ cm}^3(\text{STP}) \text{ min}^{-1}$ and ambient pressure (1 atm) over the membrane for a period of several days. The content of SO_2 in the mixed gas was adjusted to ~10 ppm by controlling the flow rate of a 50 ppm SO_2 in N_2 calibrated gas mixture (Matheson). After the treatment, the membrane was tested in the stainless steel cell to record any performance changes due to the prolonged exposure to H_2O vapor and SO_2 .

3. Results and discussion

3.1. Aminosilicate membranes

Figs. 1–3 present the room- T $\text{CO}_2:\text{N}_2$ mixed gas separation performance of the aminosilica membranes prepared by recipes aSi-1, aSi-2 and aSi-3 in Table 1, respectively. The $\text{CO}_2:\text{N}_2$ separation factor α of membranes prepared by recipe aSi-1 was initially low (<10), but increased drastically to ~50 with increasing feed humidity content, indicating the presence of a population of larger micropores of size 4–6 Å. Membranes prepared by recipe aSi-2 exhibited better sep-

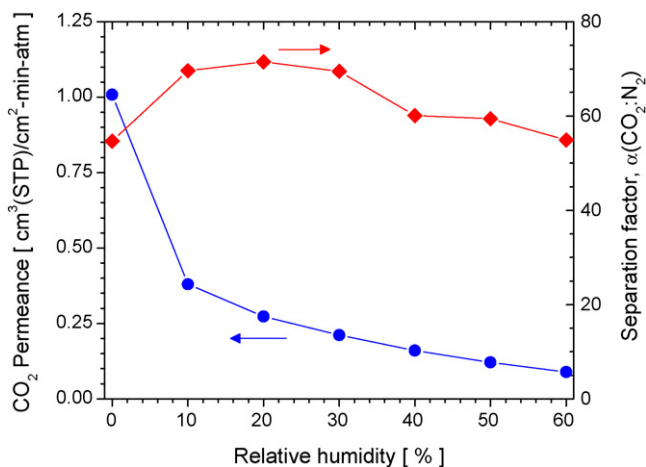


Fig. 2. Mixed gas separation performance at 25 °C of a tubular aminosilica membrane prepared with recipe aSi-2. The feed was a 10:90 (v/v) $\text{CO}_2:\text{N}_2$ mixture.

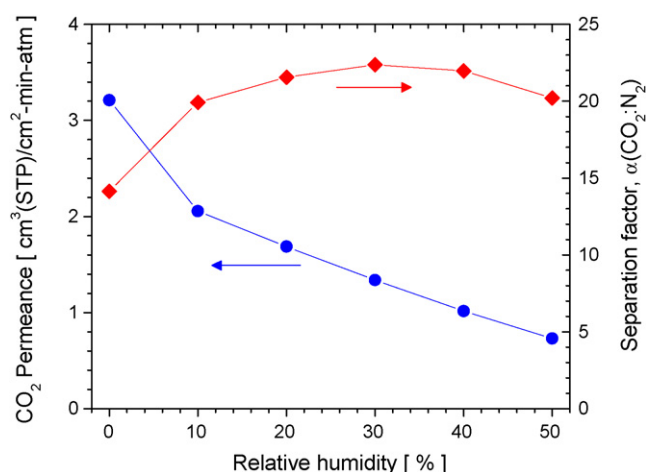


Fig. 3. Mixed gas separation performance at 22 °C of an Anodisk-supported aminosilica membrane prepared with recipe aSi-3. The feed was a 50:50 (v/v) $\text{CO}_2:\text{N}_2$ mixture.

aration performance with dry feeds and increasing feed humidity had less pronounced improvement in α . This indicates that these membranes comprised primarily of ultramicropores of size <4 Å. However, the CO_2 permeance of these membranes was relatively low (<1 MPU) compared to the aSi-1 membranes.

On the other hand, membranes aSi-3 prepared on Anodisk showed much higher CO_2 permeance and moderate α that were less sensitive to the feed humidity content. These membranes possess a wider pore size distribution with significant portion of mesopores since under the particular synthesis conditions the fast condensation reactions in the aminosilicate sol result in nanostructures with fractal dimension closer to 3, which are not suitable for achieving molecular-sized pores for gas separation [25].

For both the aSi-1 and aSi-2 membranes, the CO_2 and N_2 permeances decreased rapidly and continuously with increasing feed humidity, while α increased initially and quickly reached a maximum at a feed relative humidity of 20–30%. The observed permeance and α changes as a result of increasing feed humidity content can be explained by: (a) the pore blocking effect of H_2O on the transport of CO_2 and N_2 through the less selective large micropores; (b) the higher pore surface occupancy of H_2O in the ultramicropores (at 25 °C H_2O alone occupies roughly about 70% of the pore surface at feed RH=20%); and (c) the enhanced adsorption of CO_2 on the pore wall due to the more favorable interactions with the amine groups in the presence of H_2O and the reduction in surface coverage available for sorption and diffusion of N_2 [20].

The results in Figs. 1–3 suggest that it is difficult to achieve combined high (>1.5 MPU) CO_2 permeance and high (>50) α with the aminosilicate membranes explored in this study. Incorporation of amine groups in the silica matrix may enhance the membrane affinity for CO_2 but on the other hand may increase the effective pore size by preventing efficient interpenetration and packing of dendritic nanoclusters during xerogel drying and condensation [20]. Reducing the $\text{H}_2\text{O}:\text{Si}$ molar ratio in the case of the aSi-2 membranes resulted in better cluster packing but the porosity of the membrane was lower and hence the membrane showed lower CO_2 permeance (<1 MPU). Finally, reducing the $\text{H}^+:-\text{NH}_2$ molar ratio resulted in remarkable pore size and porosity increase for the aSi-3 membranes.

It is noted that in our earlier study [20] we could achieve $\alpha > 50$ with membranes prepared by recipe aSi-1, but in this case we used a mesoporous sublayer with smaller pore size (~10–15 Å). However, this type of sublayer may not show good long term structural stability under flue gas conditions, so we have adopted a protocol based

Table 2

CO₂:N₂ separation performance at 25 °C of fresh tubular pure silica membranes prepared by recipes Si-1 and Si-2.

Sample	Sol recipe	CO ₂ permeance, MPU [cm ³ (STP)cm ⁻² min ⁻¹ atm ⁻¹]	Separation factor [CO ₂ :N ₂]
M1	Si-1	2.5	50.4
M2	Si-2	2.6	52.7
M3	Si-2	1.4	48.6
M4	Si-2	2.0	78.4
M5	Si-2	1.7	57.0
M6	Si-2	2.4	44.5
M7	Si-2	2.2	59.7
M8	Si-1 [24]	11.3	4.1

The feed was a 10:90 (v/v) CO₂:N₂ mixture. Sample M8 was prepared with molar ratio H⁺:Si = 0.085 in the precursor silica sol.

on the Brij56 surfactant which results in more stable cubic-ordered mesoporous structures [26].

3.2. Pure silica membranes

Membranes prepared without amine groups showed better performance for CO₂:N₂ separation, as shown by the results summarized in Table 2. The critical factor that affected membrane pore structure and hence CO₂:N₂ separation performance was the H⁺:Si molar ratio of the precursor silica sol. In this study, we adjusted this ratio to 1/10 of the value used by previous workers [24] in order to obtain satisfactory separation performance with the present support and preparation protocol. For comparison, sample M8 in Table 2 and Fig. 4 prepared according to [24] showed much higher CO₂ permeance and lower α compared to the rest of the samples. This sample exhibited a detectable SF₆ permeance of ~0.1 MPU, suggesting the presence of a broad distribution of micropores of sizes up to 5–6 Å that give rise to higher permeance but moderate CO₂:N₂ selectivity.

Fig. 5 shows the CO₂:N₂ mixed gas separation performance of sample M4 in the temperature range of 25–100 °C. As seen in the figure, the permeance of CO₂ increases moderately while that of N₂ increases more drastically as a result of activated diffusion, resulting in a fast α decline. This behavior was reversible with temperature cycling and typical of all membrane samples prepared in this study under similar conditions. In order to reduce the fast decline of α at elevated T , we performed membrane calcination at progressively higher T (up to 500 °C) in order to densify the membrane framework and reduce its pore size [24], but this treatment did not prove effective in our case. However, as seen in Fig. 6, the presence of humidity

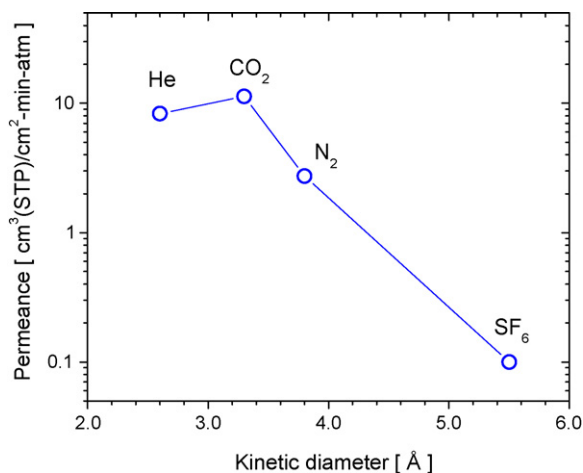


Fig. 4. Molecular sieving behavior of membrane M8 in Table 2 prepared according to Ref. [20].

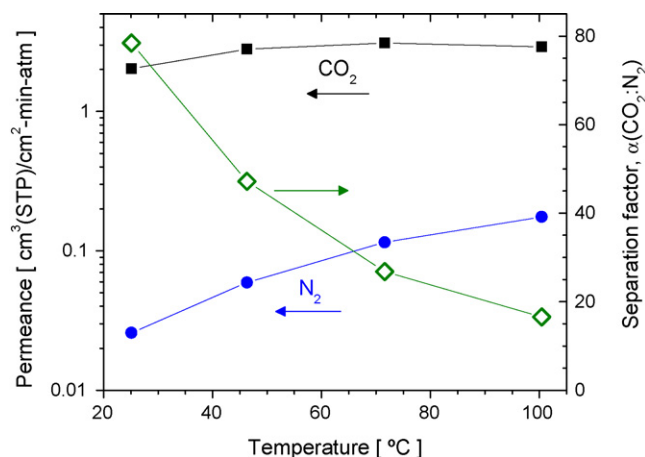


Fig. 5. Mixed gas separation performance at 25–100 °C of a tubular silica membrane prepared with recipe Si-2. The feed was a 10:10:80 (v/v) CO₂:N₂:He mixture.

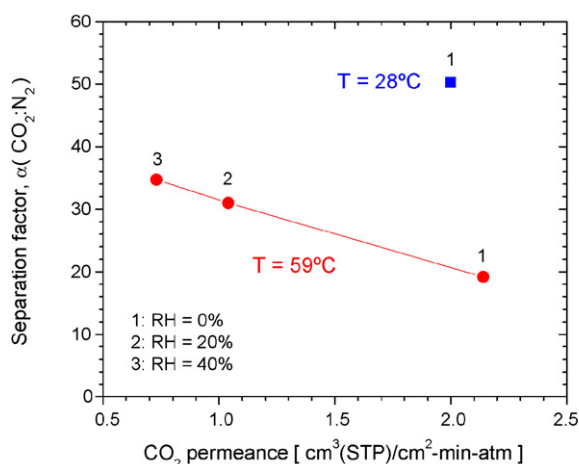


Fig. 6. Plot of separation factor α (CO₂:N₂) vs. CO₂ permeance for increasing feed humidity content, for a tubular silica membrane prepared with recipe Si-2. The feed was a 20:80 (v/v) CO₂:N₂ mixture.

in the feed aids in improving α at elevated T but at the expense of CO₂ permeance, as was also observed with the aminosilicate membranes in Figs. 1–3.

3.3. Ni-doped silica membranes

Ni-doped membranes were also prepared in this study because of their potential to resist densification under the flue gas conditions involving H₂O vapor and SO₂ impurity gas [27–29]. Table 3 shows the room- T CO₂:N₂ mixed gas separation performance of Ni-doped silica membranes prepared with a molar ratio Ni:Si = 0.1. These membranes in general exhibit higher CO₂ permeance and lower α compared to the pure silica membranes prepared under

Table 3

CO₂:N₂ separation performance at 25 °C of fresh tubular Ni-doped silica membranes prepared by a modified Si-2 recipe. The feed was a 10:90 (v/v) CO₂:N₂ mixture.

Sample	Ni:Si ratio	CO ₂ permeance, MPU [cm ³ (STP)cm ⁻² min ⁻¹ atm ⁻¹]	Separation factor [CO ₂ :N ₂]
N1	0.1	4.56	21.9
N2	0.1	3.15	19.2
N3	0.1	4.92	16.4
N4	0.1	5.96	21.7
N5	0.2	0.58	92.0

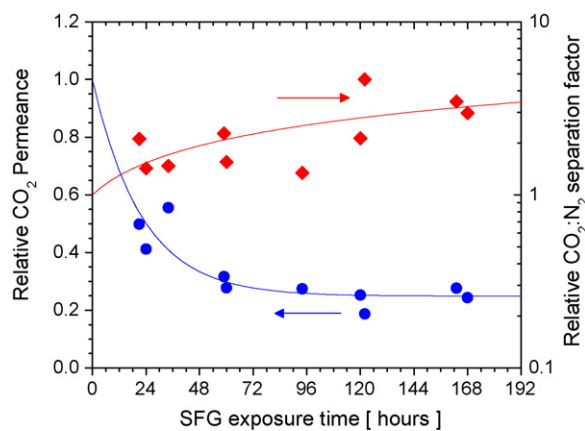


Fig. 7. Changes in CO_2 permeance and separation factor $\alpha(\text{CO}_2:\text{N}_2)$ as a function of exposure time to SFG conditions for different (pure and Ni-doped) tubular silica membranes. The separation performance was measured with a 10:90 (v/v) $\text{CO}_2:\text{N}_2$ feed at 25 °C before and after the indicated exposure time.

comparable conditions. We also prepared membranes with molar ratio Ni:Si=0.2 but the separation performance of these samples was less reproducible. Some samples would exhibit low CO_2 permeance (<1 MPU) combined with high α (close to 100), whereas other samples showed $\alpha < 10$, implying the presence of film defects. For this reason, we focused our attention on the membranes prepared with molar ratio Ni:Si=0.1, since these membranes have higher initial (fresh) porosity and/or pore size and hence they have better potential to resist densification during prolonged exposure to SFG conditions.

3.4. Membrane stability under SFG conditions

The $\text{CO}_2:\text{N}_2$ mixed gas separation performance of pure and Ni-doped silica membranes was studied after several days of exposure to SFG conditions in order to assess the impact of H_2O vapor and trace SO_2 gas on the membrane pore structure. Fig. 7 shows the overall effect of SFG exposure time on membrane CO_2 permeance and $\text{CO}_2:\text{N}_2$ separation factor. As seen in the figure, the CO_2 permeance decreases rapidly in the first 24–48 h of exposure and then stabilizes at about 25% of its original level after prolonged exposure. The reduction in CO_2 permeance is accompanied by different levels of improvement in $\alpha(\text{CO}_2:\text{N}_2)$, depending on the initial absolute membrane permeance and the presence of Ni dopant in the microstructure.

Figs. 8 and 9 show the separation performance of a pure silica membrane after 60 and 120 h exposure to SFG conditions, respectively. From these figures we observe that a 50% reduction in CO_2 permeance with only 15% increase in α occurs when the exposure time to SFG conditions increases from 60 to 120 h. On the other hand, the Ni-doped silica membrane studied in Fig. 10 maintains higher CO_2 permeance and higher α even after 168 h exposure to SFG conditions. The stabilizing effect of Ni can be explained by the enhanced porosity of the doped membranes and the reduction in the rate of condensation reactions between neighboring $-\text{Si}-\text{OH}$ units in the silica framework due to the presence of Ni oxide. This stabilizing effect of metal oxide doping on the pore structure of sol-gel derived nanostructured ceramics was established in previous studies with a variety of guest metal atoms such as La, Y, Mg, and Al on both the xerogel and the thin film form of alumina, titania, zirconia and silica membranes [30,31].

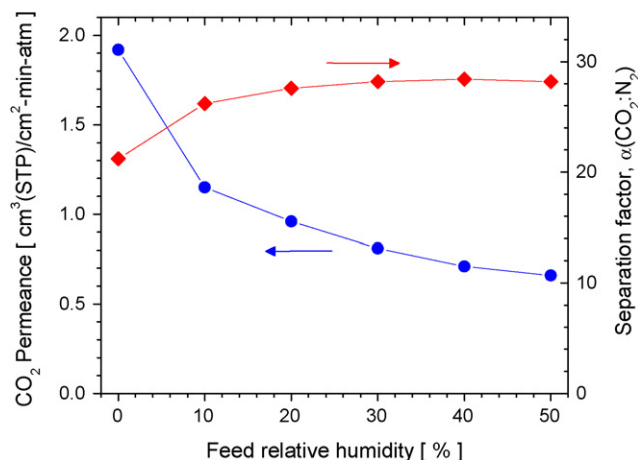


Fig. 8. Mixed gas separation performance at 62 °C of a tubular pure silica membrane prepared with recipe Si-2. The membrane was exposed for 60 h in SFG conditions. The feed was a 10:90 (v/v) $\text{CO}_2:\text{N}_2$ mixture.

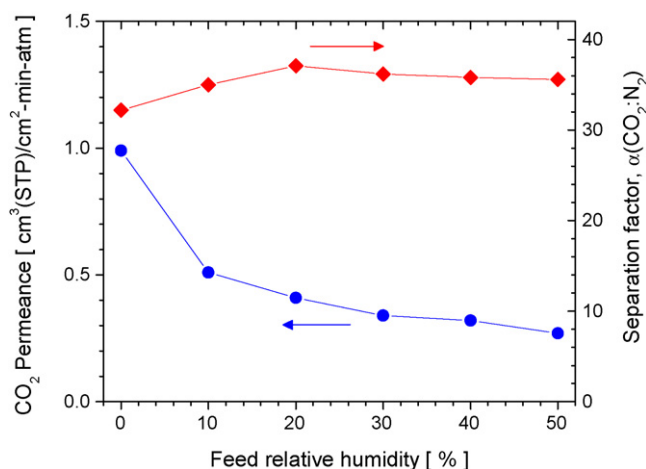


Fig. 9. Mixed gas separation performance at 65 °C of the tubular pure silica membrane shown in Fig. 8. The membrane was exposed for additional 60 h (total 120 h) in SFG conditions. The feed was a 10:90 (v/v) $\text{CO}_2:\text{N}_2$ mixture.

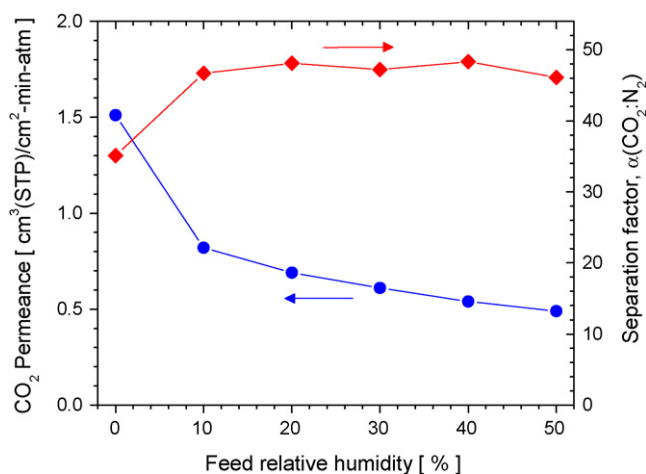


Fig. 10. Mixed gas separation performance at 56 °C of a tubular Ni-doped silica membrane. The membrane was exposed for 163 h in SFG conditions. The feed was a 10:90 (v/v) $\text{CO}_2:\text{N}_2$ mixture.

3.5. Future directions

As seen in Fig. 10, although the Ni-doped silica membrane maintains high α at elevated T , its CO_2 permeance is still significantly lower than the level necessary (e.g. >2 MPU) for large-scale application of the membrane in power plant flue gas CO_2 capture. We attempted to improve the CO_2 permeance of these membranes by diluting the precursor Ni-doped silica sol with ethanol prior to membrane deposition in order to decrease membrane thickness, but this resulted in reduced α , suggesting that a fundamentally different approach is necessary to prepare silica membranes meeting the stringent separation performance and stability requirements for large-scale flue gas CO_2 capture.

An alternative technique that can potentially allow the preparation of molecular sieving silica membranes combining high CO_2 permeance (>2 MPU) and high α (>50) is atomic layer deposition (ALD). The advantage of this technique is that it allows monolayer-by-monolayer growth of a metal oxide thin film on a suitable support by cycling contact of the metalorganic and water vapor reactants with the film surface, thus allowing molecular level control of the film thickness and nanostructure [32]. Recently we demonstrated successful introduction of attractive molecular sieving properties on mesoporous silica films supported on anodic alumina disks by a plasma-modified ALD technique [33]. Currently we are working on extending this approach on tubular supports for the purpose of preparing high permeance, high α molecular sieve silica membranes that would be suitable for power plant flue gas capture. Other than reducing membrane thickness, the ALD technique also offers improved flexibility for derivatizing the membrane with amine groups while overcoming the gelation issues associated with the traditional liquid phase sol–gel processing.

4. Conclusions

We have explored three types of silica-based, tubular microporous membranes for CO_2 : N_2 separation under simulated flue gas conditions. Amine-derivatized silica membranes could not achieve combined high (>50) α and high (>1 MPU) CO_2 permeance, most likely because of the difficulty in independently controlling the pore size and porosity of the aminosilicate framework. Pure silica membranes prepared under optimized conditions showed the best combination of high (1.5–2.0 MPU) CO_2 permeance and high (50–80) CO_2 : N_2 separation factor, but α decreased drastically with increasing operating temperature. These membranes showed gradual decline in permeance as a result of prolonged exposure to SFG conditions due to densification and shrinkage of the framework induced by H_2O vapor and trace SO_2 gas. Doping the membrane with nickel oxide mitigated the densification due to enhancement in porosity and reduction in condensation reactions in the doped silicate framework during operation. Despite the improvement in performance imparted by metal oxide doping, the permeance of the membranes still needs to be improved to be attractive for power plant scale CO_2 capture.

Acknowledgements

This work was supported by the Department of Energy's National Energy Technology Laboratory (www.netl.doe.gov) under grant #DE-FG26-04NT42120. We are grateful to Mr. José Figueroa and other members of NETL's staff for useful technical discussions during the course of this project. Sandia is a multiprogram laboratory operated by Sandia Corporation, a Lockheed–Martin Company, for the United States Department of Energy's National Nuclear Security Administration under Contract DE-AC04-94AL85000.

References

- [1] R.W. Baker, Future directions of membrane gas separation technology, *Ind. Eng. Chem. Res.* 41 (2002) 1393.
- [2] B.D. Freeman, Basis of permeability/selectivity tradeoff relations in polymeric gas separation membranes, *Macromolecules* 32 (1999) 375.
- [3] W.J. Koros, R. Mahajan, Pushing the limits on possibilities for large scale gas separations: which strategies? *J. Membr. Sci.* 175 (2000) 181.
- [4] R. Bredeken, K. Jordal, O. Bolland, High-temperature membranes in power generation with CO_2 capture, *Chem. Eng. Proc.* 43 (2004) 1129.
- [5] R. Bounaceur, N. Lape, D. Roizard, C. Vallieres, E. Favre, Membrane processes for post-combustion carbon dioxide capture: a parametric study, *Energy* 31 (2006) 2220.
- [6] E. Favre, Carbon dioxide recovery from post-combustion processes: can gas permeation membranes compete with absorption? *J. Membr. Sci.* 294 (2007) 50.
- [7] C.E. Powell, G.G. Qiao, Polymeric CO_2 / N_2 gas separation membranes for the capture of carbon dioxide from power plant flue gases, *J. Membr. Sci.* 279 (2006) 1.
- [8] P.K. Gantzel, U. Merten, Gas separations with high flux cellulose acetate membranes, *Ind. Eng. Chem. Proc. Des. Dev.* 9 (1970) 331.
- [9] Y.S. Lin, I. Kumakiri, B.N. Nair, H. Alsayouri, Microporous inorganic membranes, *Sep. Purif. Methods* 31 (2002) 229.
- [10] K. Kusakabe, T. Kuroda, S. Morooka, Separation of carbon dioxide from nitrogen using ion-exchanged faujasite-type zeolite membranes formed on porous support tubes, *J. Membr. Sci.* 148 (1998) 13.
- [11] H.B. Park, Y.K. Kim, J.M. Lee, S.Y. Lee, Y.M. Lee, Relationship between chemical structure of aromatic polyimides and gas permeation properties of their carbon molecular sieve membranes, *J. Membr. Sci.* 229 (2004) 117.
- [12] M. Noack, P. Kölsch, R. Schäfer, P. Toussaint, Jürgen Caro, Molecular sieve membranes for industrial applications: problems, progress, solutions, *Chem. Eng. Technol.* 25 (2002) 221.
- [13] H. Verweij, Y.S. Lin, J. Dong, Microporous silica and zeolite membranes for hydrogen purification, *MRS Bull.* 31 (2006) 756.
- [14] Y. Gu, S.T. Oyama, High molecular permeance in a poreless ceramic membrane, *Adv. Mater.* 19 (2007) 1636.
- [15] C.Y. Tsai, S.Y. Tam, Y. Lu, C.J. Brinker, Dual-layer asymmetric microporous silica membranes, *J. Membr. Sci.* 169 (2000) 255.
- [16] Y. Lu, G. Cao, R.P. Kale, S. Prabakar, G.P. López, C.J. Brinker, Microporous silica prepared by organic templating: relationship between the molecular template and pore structure, *Chem. Mater.* 11 (1999) 1223.
- [17] G. Xomeritakis, S. Naik, C.M. Braunbarth, C.J. Cornelius, R. Pardey, C.J. Brinker, Organic-templated silica membranes. I. Gas and vapor transport properties, *J. Membr. Sci.* 215 (2003) 225.
- [18] J.H. Moon, H. Ahn, S.H. Hyun, C.H. Lee, Separation characteristics of tetrapropyl-ammonium bromide templating silica/alumina composite membrane in CO_2 / N_2 , CO_2 / H_2 and CH_4 / H_2 systems, *Kor. J. Chem. Eng.* 21 (2004) 477.
- [19] J.H. Moon, Y.J. Park, M.B. Kim, S.H. Hyun, C.H. Lee, Permeation and separation of a carbon dioxide/nitrogen mixture in a methyltriethoxysilane templating silica/ α -alumina composite membrane, *J. Membr. Sci.* 250 (2005) 195.
- [20] G. Xomeritakis, C.Y. Tsai, C.J. Brinker, Microporous sol–gel derived aminosilicate membrane for enhanced carbon dioxide separation, *Sep. Purif. Technol.* 42 (2005) 249.
- [21] B.A. McCool, W.J. DeSisto, Amino-functionalized silica membranes for enhanced carbon dioxide permeation, *Adv. Funct. Mater.* 15 (2005) 1635.
- [22] T.A. Peters, J. Fontalvo, M.A.G. Vorstman, N.E. Benes, R.A. van Dam, Z.A.E.P. Vroon, E.L.J. van Soest-Vercammen, J.T.F. Keurentjes, Hollow fibre microporous silica membranes for gas separation and pervaporation. Synthesis, performance and stability, *J. Membr. Sci.* 248 (2005) 73.
- [23] G. Xomeritakis, N.G. Liu, Z. Chen, Y.B. Jiang, R. Köhn, P.E. Johnson, C.Y. Tsai, P.B. Shah, S. Khalil, S. Singh, C.J. Brinker, Anodic alumina supported dual-layer microporous silica membranes, *J. Membr. Sci.* 287 (2007) 157.
- [24] R.M. de Vos, H. Verweij, Improved performance of silica membranes for gas separation, *J. Membr. Sci.* 143 (1998) 37.
- [25] C.J. Brinker, R. Sehgal, S.L. Hietala, R. Deshpande, D.M. Smith, D. Loy, C.S. Ashley, Sol–gel strategies for controlled porosity inorganic materials, *J. Membr. Sci.* 94 (1994) 85.
- [26] H. Fan, C. Hartshorn, T. Buchheit, D. Tallant, R. Assink, R. Simpson, D.J. Kissel, D.J. Lacks, S. Torquato, C.J. Brinker, Modulus–density scaling behaviour and framework architecture of nanoporous self-assembled silicas, *Nat. Mater.* 6 (2007) 418.
- [27] M. Kanezashi, M. Asaeda, Stability of H_2 -permselective Ni-doped silica membranes in steam at high temperature, *J. Chem. Eng. Jpn.* 38 (2005) 908.
- [28] M. Kanezashi, T. Fujita, M. Asaeda, Nickel-doped silica membranes for separation of helium from organic gas mixtures, *Sep. Sci. Technol.* 40 (2005) 225.
- [29] M. Kanezashi, M. Asaeda, Hydrogen permeation characteristics and stability of Ni-doped silica membranes in steam at high temperature, *J. Membr. Sci.* 271 (2006) 86.
- [30] Y.S. Lin, C.H. Chang, R. Gopalan, Improvement of thermal stability of porous nanostructured ceramic membranes, *Ind. Eng. Chem. Res.* 33 (1994) 860.

- [31] G.P. Fotou, Y.S. Lin, S.E. Pratsinis, Hydrothermal stability of pure and modified microporous silica membranes, *J. Mater. Sci.* 30 (1995) 2803.
- [32] Y.B. Jiang, N. Liu, H. Gerung, J.L. Cecchi, C.J. Brinker, Nanometer-thick conformal pore sealing of self-assembled mesoporous silica by plasma-assisted atomic layer deposition, *J. Am. Chem. Soc.* 128 (2006) 11018.
- [33] Y.B. Jiang, G. Xomeritakis, Z. Chen, D. Dunphy, D.J. Kessel, J.L. Cecchi, C.J. Brinker, Sub-10 nm thick microporous membranes made by plasma-defined atomic layer deposition of a bridged silsesquioxane precursor, *J. Am. Chem. Soc.* 129 (2007) 15446.